Biosensors and Bioelectronics 59 (2014) 6–13

Contents lists available at ScienceDirect

Biosensors and Bioelectronics

journal homepage: www.elsevier.com/locate/bios

Direct electrochemical detection of PB1-F2 protein of influenza A virus in infected cells

Anna Miodek [a], Helene Sauriat-Dorizon [a], Christophe Chevalier [b], Bernard Delmas [b], Jasmina Vidic [b,*], Hafsa Korri-Youssoufi [a,**]

[a] CNRS UMR-8182, Institut de Chimie Moléculaire et de Matériaux d'Orsay, Equipe de Chimie Bioorganique et Bioinorganique, Bâtiment 420, 91405 Orsay, France
[b] INRA, Unité de Virologie et Immunologie Moléculaires, UR892, Domaine de Vilvert, F-78350, Cntre de Jouy-en-Josas, France

ARTICLE INFO

Article history:
Received 6 December 2013
Received in revised form
6 February 2014
Accepted 14 February 2014
Available online 26 February 2014

Keywords:
Influenza virus
Immunosensor
Electrochemical
Biosensor
Ferrocene
Polypyrrole

ABSTRACT

Influenza virus represents a major concern of human health and animal production. PB1-F2 is a small proapoptotic protein supposed to contribute to the virulence of influenza A virus (IAV). However, the molecular mechanism of action of PB1-F2 is still unclear.PB1-F2 expression and behavior during the viral cycle is difficult to follow with classical biochemical methods. In this work we have developed an electrochemical biosensor based on immuno-detection system for quantification of PB1-F2 protein in infected cell. The electrochemical immunosensor was based on conducting copolypyrrole integrating ferrocenyl group as redox marker for enhancing signal detection. A specific anti-PB1-F2 monoclonal antibody was immobilized on the copolypyrrole layer via biotin–streptavidin system. We demonstrate that this electrochemical system sensitively detect purified recombinant PB1-F2 over a wide range of concentrations from 5 nM to 1.5 μM. The high sensor sensitivity allowed the detection of PB1-F2 in lysates of infected cells confirming that PB1-F2 is expressed in early stages of viral cycle. The immunosensor developed shows enhanced performances for the evaluation of PB1-F2 protein concentration in biological samples and could be applied for studying of PB1-F2 during influenza virus infection.

1. Introduction

Influenza A virus (IAV) constitutes a major problem of human health since IAV affects millions of people each year. The primary reservoir of IAV is aquatic birds. Some avian strains can infect human and other mammals either directly or after a genetic reassortment which creates human-avian strains. Most human-avian strains have pandemic potential. It has be the case in 1918 when the most fatal pandemic of modern history of Spanish flu virus killed approximately 50 million of people. The last reported human cases of H7N9 virus infections evidenced the need of constant survey and evaluation of the public health risk of newly emerging strains of IAV.

IAV belongs to the *Orthomyxoviridae* family and has a negative-sens RNA genome segmented into eight strands. Each segment encodes one protein (PB2, HA, NP, NA) or two proteins (PA/PA-X, M1/M2, NSA/NS2), while PB1 segment encodes three different proteins (PB1/PB1-F2/N40). The virulence of the virus is complex and can be influenced by each of the viral segment, but mostly encoding HA, NA, NS, PA and PB1 (Palese, 1977; Chen et al., 2001; Wise et al., 2011; Yewdell and Ince, 2012). Although expression of PB1-F2 is not necessary for developing an influenza infection, this protein was reported to contribute to the immunopathological disorders developed during infection (Le Goffic et al., 2010, 2011). PB1-F2 was reported to regulate polymerase activity, induce apoptosis, and contribute to susceptibility to secondary bacterial infection. However, the exact mechanism and the direct implication of PB1-F2 in virulence remain unclear.

PB1-F2 is a small protein of 87–90 amino acids which is expressed in most human and avian IAV strains in its full-length version. PB1-F2 is considered as an intrinsically disordered protein since PB1-F2 is non-structured in native state but can switch from alpha-helix to beta-sheet conformation depending upon its environment. Furthermore, PB1-F2 has no secondary structure in aqueous solutions but adopts beta-sheet conformation and forms amyloid fibers in a membrane mimicking environment (Chevalier et al., 2010). PB1-F2 amyloid fibers were, also, detected in infected cells at the membrane vicinity. Protein PB1-F2 is expressed independently of the expression level of others influenza proteins and supposed to have a short half-life since is hardly detectable in detergent infected-cell lysate (Chen et al., 2001, Le Goffic et al., 2010). However, these previous studies suggested that classical biochemical methods were not fully adapted to follow PB1-F2

* Corresponding author. Tel.: +33 169 15 7440; fax: +33 1 69157281.
** Corresponding author. Tel.: +33 1 34 65 26 23; fax: +33 134652621.
E-mail addresses: jasmina.vidic@jouy.inra.fr (J. Vidic), hafsa.korri-youssoufi@u-psud.fr (H. Korri-Youssoufi).

http://dx.doi.org/10.1016/j.bios.2014.02.037
0956-5663/

expression during the viral cycle. Thus a new detection method for PB1-F2 quantification in biological samples is needed.

Among various techniques for detection of viral proteins, electrochemical biosensors are promising tools. Different methods for detection can be used such as impedance (Kukol et al., 2008; Wang et al., 2009), differential pulse voltammetry (Zhu et al., 2009; Liu et al., 2011), cyclic voltammetry (Kamikawa et al., 2010; Chung et al., 2011) and conductivity (Tam et al., 2009, Kao et al., 2011). Regarding literature data, various electrochemical biosensors have been developed for detection of influenza virus based on specific DNA sequences (Kukol et al. 2008; Zhu et al., 2009) or on detection of surface proteins such as hemagglutinin (HA) (Wang et al., 2009; Kamikawa et al., 2010) or neuraminidase (NA) (Lum et al., 2012). Electrochemical biosensors pose an attractive solution for integration into microscale devices because they require minimal instrumentation; they are scalable and readily integrated with microelectronics. For instance, electrochemical patterning and detection of multiple DNA of H5N1 virus sequences have been developed (Pavlovic et al., 2008). Portable impedance biosensor for detection of avian influenza virus by immunodetection of HA protein was proposed by (Wang et al., 2011).

Here we report for the first time the development of an electrochemical immunosensor for detection of viral protein PB1-F2 in infected cell during viral cycle. The immunosensor is based on the immobilization of specific anti-PB1-F2 antibody on the surface of the gold microelectrode modified with conducting polypyrrole bearing ferrocene as a redox marker. Biotinylated anti-PB1-F2 antibody was successfully grafted on the electrode surface through biotin/streptavidin system. The biosensor construction was characterized by electrochemical measurements, Surface Plasmon Resonance (SPR) and Atomic Force Microscopy (AFM) techniques. It allows the quantification of purified PB1-F2 and determination of PB1-F2 expression level in IAV infected cells. Results revealed a maximum PB1-F2 expression level at 8 h post-infection in A549 alveolar epithelial cells.

2. Materials and methods

2.1. Purification of PB1-F2 protein.

Full-length PB1-F2 His-tag gene of A/WSN/1933 (H1N1) influenza virus was cloned in the *Escherichia coli* expression vector pET-22b+ and expressed in the BL-21 Rosetta DE3 *E. coli* strain. After induction in isopropyl β-D-1-thiogalactopyranoside (IPTG), PB1-F2 was purified as described previously (Chevalier et al., 2010). Briefly, the transformed cells were pelleted by centrifugation and lysed by sonication in 50 mM Tris–HCl, pH 7.5, 10 mM EDTA buffer containing 0.1% Triton X100. The lysate was centrifuged during 30 min at 10,000 g at 4 °C to collect inclusion bodies. The inclusion bodies were solubilized overnight under agitation in 8 M urea, 0.5 M NaCl, 5 mM imidazole, 20 mM Tris–HCl buffer, pH 8, at 4 °C. The lysate was clarified by centrifugation during 30 min at 10,000 g at 4 °C and the supernatant was collected and loaded on a Hitrap-IMAC column using the AKTA Purifier-100 FPLC chromatographic system (GE Healthcare). After this first step of purification the fractions containing PB1-F2 were pooled and further purified using size-exclusion chromatography on a Sepharose S200 column. Purified PB1-F2 His-Tag protein was lyophilized and stored at −20 °C. Prior to analysis lyophilized protein powder was dissolved in 10 mM sodium-acetate buffer, pH 5.

2.2. Cell culture and viral infection

The human alveolar epithelial cell line A549 was purchased from the American Type Culture Collection (Manassas, VA). Cells were propagated and maintained in RPMI 1640 medium (Lonza) supplemented with 10% fetal calf serum, 2 mM L-glutamine, 100 IU/ml penicillin and 100 μg ml^{-1} streptomycin. Cells were maintained at 37 °C in a 5% CO_2 incubator. We used influenza A/WSN/1933 (H1N1) in this study. Viral stocks of wild-type (WT) and PB1-F2 knockout virus mutant (F2) were produced as previously described (Chevalier et al., 2010; Le Goffic et al., 2011). For infections, cells were washed with fetal calf serum-free medium and incubated with influenza viruses at 0.1 multiplicity of infection for 1 h at 37 °C. Infected cells were then incubated at 37 °C with complete fetal calf serum until collection.

2.3. Antibodies modification.

Rabbit hybridoma monoclonal anti-PB1-F2 (Ab R14) antibodies were kind gifts from Dr J.F. Vautherot (INRA). The antibodies were produced against the full-length PB1-F2 His-tag. Ab R14 was biotinylated using DSB-X™ Biotin Protein Labeling Kit (Molecular Probes, US). The affinity of the R14 antibody to PB1-F2 was tested with recombinant proteins using SPR measurement. The Kd value of R14 to recombinant PB1-F2 was calculated to 0.2 μM.

2.4. Reagents

The modified monomer pyrrole 1-(phthalimidylbutanoate)-1′-(*N*-(3-butylpyrrole)butanamide) ferrocene (PyFcNHP), was synthesized by coupling the 1,1′-(phthalimidylbutanoate)-ferrocene ($Fc(NHP)_2$) with the 2-(3-pyrrole) butylamine prepared according to the procedure described in supporting information (see Supplementary data). Pyrrole (Py) was purchased from Sigma-Aldrich and distilled under argon before use. Biotin hydrazide and streptavidin were purchased from Sigma-Aldrich. Analysis were performed in phosphate buffer saline (PBS) pH 7.4 containing 10 mM Na_2HPO_4, 1.8 mM KH_2PO_4, 2.7 mM KCl and 137 mM NaCl or 5 mM sodium acetate buffer pH 5. The buffers were filtered by membrane 0.22 μm before use.

2.5. Electrochemical measurement

Electrochemical measurements were performed using a potentiostat Autolab PGSTAT 12 (Metrohm, France) controlled by GPES software and a portative potentiostat Autolab PGSTAT 101 controlled by Nova software. Electrochemical cell for electropolymerization was constituted of two-compartments and was purchased from BASi Analytical Instruments. The measuring cell was composed of a gold disc of 2.01×10^{-2} cm^2 as a working electrode and the platinum wire as an auxiliary electrode. These two electrodes were separated from the Ag/AgCl electrode as reference. The all electrodes used for electrochemical experiment are also from BASi Analytical Instruments. Cyclic voltammetry (CV) was performed in the range of potential from −0.4 to 0.6 V with scan rate of 100 mV s^{-1}. Differential pulse voltammetry (DPV) was performed in the range of potential −0.6 to 0.6 V with the modulation amplitude of 50 mV and the step potential of 5 mV.

2.6. Electropolymerization

The copolymer film was grown on the gold surface in acetonitrile solution containing 0.5 M $LiClO_4$ and a mixture of Py and PyFcNHP monomers at concentration ratio of 8:2 mM respectively. The electropolymerization was performed by cycling the potential from −0.4 V to 0.95 V with a scan rate of 100 mV s^{-1}. The reaction was stopped when the reduction current intensity of ferrocene reached 30 μA which corresponds approximately to 14 cycles. These conditions were chosen after optimization step and in order to obtain the thin layer of copolymer with intense and reproducible electrochemical signal. The modified gold electrode obtained was washed with acetonitrile and with double distilled water.

2.7. Construction of biosensor

The schematic illustration of the biosensor elaboration is given in Fig. 1. Each step of the biosensor construction was performed by placing 40 μl of analyte in 10 mM PBS buffer solution pH 7.4 on the surface of the working electrode at room temperature. The biosensor was constructed by consecutively adding 40 μl biotin hydrazide (2 mg mL^{-1}) during 45 min, then 40 μl streptavidin (100 μl mL^{-1}) during 45 min and finally 40 μl biotinylated Ab R14 (8 μg mL^{-1}) during 45 min on the surface of the working electrode at room temperature. The modified film was washed with water and PBS buffer to eliminate the residues non-bonded on the surface after each step of the biosensor construction. Before protein detection, biosensor was stabilized in 5 mM sodium acetate buffer pH 5 at 4 °C overnight. After this step the electrochemical response of the biosensor remains stable. The stability of electrochemical response of biosensors was studied during two weeks where no significant variation was observed.

2.8. Detection of recombinant PB1-F2

Detection of the recombinant PB1-F2 protein was performed by dipping the biosensor in PB1-F2 preparation in 5 mM sodium acetate buffer, pH 5, for 40 min at 25 °C. The buffer solution as selected to maintain PB1-F2 stable in monomeric form even for high concentration. Protein concentration ranged from 5 nM to 5000 nM was measured. After incubation, the biosensor was washed with sodium acetate buffer to eliminate proteins non-linked. This measurement was performed by successive incubation of biosensors in various PB1-F2 concentrations. To check the reproducibility the experiment was repeated three times with freshly prepared biosensors.

2.9. Detection of PB1-F2 in IAV-infected cells.

At different time post infection, IAV-infected A549 cells were collected centrifuged and the pellets were frozen at −80 °C. The pellets were then suspended in 5 mM sodium acetate buffer pH 5. The concentrations of the total protein extracts were estimated with the NanoDrop 2000C UV–vis spectrophotometer (thermo Scetific, France) and the BCA reagent (Pierce, Brebiers, France) with BSA as a standard. The concentration of protein was adjusted to 100 μg ml^{-1}. Non-infected cells (NI) and PB1-F2 knock-out F2-infected cells were used as negative controls. Detection was performed by dipping the biosensor in cell lysate preparations for 40 min at 25 °C. To analyze the reproducibility of the experiments with cell, the detection was repeated with two series of cells and each measurement of lysate was duplicated. For these experiments 120 fresh biosensors were prepared.

2.10. SPR measurements

SPR measurements were performed by Autolab ESPRIT double-channel instrument (Eco Chemie, Utrecht, The Netherlands) controlled by DA software. The instrument was associated with the

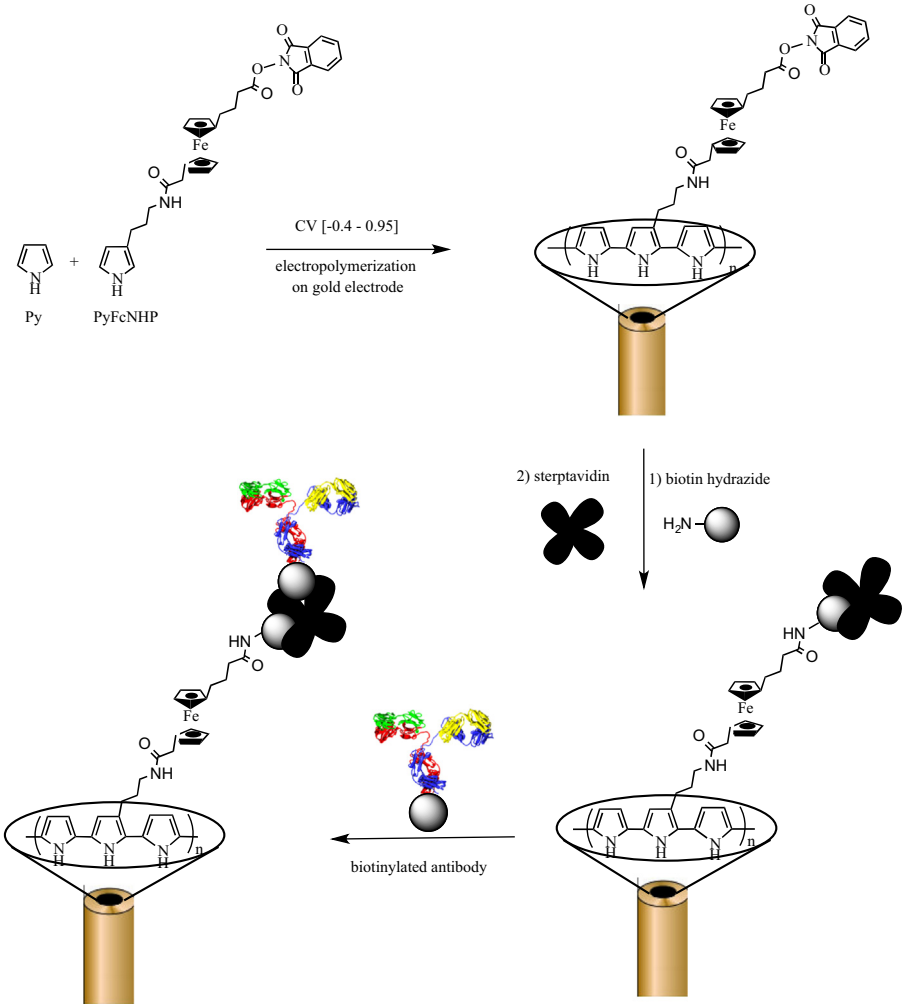

Fig. 1. Schematic diagram for biosensor construction.

electrochemical cell consist of three-electrodes system, the gold disc as a working electrode (active surface 0.06 cm^2), the platinum as a counter electrode and the Ag/AgCl as a reference electrode which were purchased from Metrohm (France).

2.11. AFM measurements

A commercial dimension 3100 (Vecco Instruments, USA) AFM was used for topographical characterization of the samples. All measurements were performed at the tapping mode using rectangular silicon AFM tip.

3. Results and discussions

3.1. Electrochemical polymerization of copoly(Py-PyFcNHP)

The copolymer film copoly(Py-PyFcNHP) was grown on gold surface by electropolymerization of two pyrrole monomers, pyrrole (Py) and a pyrrole modified with ferrocenyl group (PyFcNHP) in the ratio of 8:2 mM. PyFcNHP served to anchor the proteins at the modified surface and exhibits an intense and sensitive electrochemical signal thanks to ferrocenyl group. Py was used as a spacer to limit the steric problems on the surface which occurs during the immobilization of proteins (Lê et al., 2010a). Fig. 2A displays the electropolymerization process obtained by potential scan between −0.4 V and 0.95 V. During this reaction, two peaks of different intensities appeared at −0.05 V and 0.295 V vs Ag/AgCl. The first one is the redox signal of polypyrrole and the second corresponds to the ferrocene group as already described (Lê et al., 2010b). During each cycle of functionalization, an increase of the oxidative and reductive currents was observed for both peaks, indicating the grown of the copolymer on the surface (Fig. 2A).

The electropolymerization process was also monitored by SPR experiments (Fig. 2B). The polymerization of Py and PyFcNHP was performed by sweep potential during 14 cycles to reach a desired thickness of the layer. The SPR kinetic response demonstrates an increase in the angle after each cycle. The inset shows the changes of reflectivity before and after polymerization. The angle of resonance shifted from 69.3° to 71.2° after copoly(Py-PyFcNHP) deposition, thus giving a variation of the angle of 1.9°. These changes were attributed to the growth of the copolymer film onto the gold surface. Using Winspall's program and with fitting parameters: $n_{(prism)}=1.52$, $n_{(titanium)}=2.36+i3.11$ with $d=2.5$ nm, $n_{(gold)}=0.09+i3.82$ with $d=49$ nm, $n_{(copoly(py\text{-}pyNHP))}=1.421+0.0915i$, the thickness of the copoly(Py-PyFcNHP) film was estimated to 10 nm.

3.2. Construction and characterization of the biosensor.

The construction of the biosensor was realized by successive modification of the functionalized surface with biotin hydrazide, streptavidin and biotinylated antibody Ab R14. The characterization of the biosensor layer was performed by SPR, AFM, and electrochemical methods. Fig. 3A shows the real time SPR binding curve during the formation of the immunosensor. The SPR angle increased rapidly upon the addition of each biomolecule, corresponding both to the association step and the modification of the refractive index of the solution. After reaching the saturation for each biomolecule, the experiment was stopped and the surface was washed with the PBS buffer solution to remove non-attached molecules. The addition of biotin hydrazide modified the SPR angle of 58 m° ($\Delta\theta_1$) indicating a coupling of biotin with immobilized PyFcNHP. When streptavidin and biotinylated antibody Ab R14 were added, the SPR angle increases of 171 m° ($\Delta\theta_2$) and 48 m° ($\Delta\theta_3$) respectively, confirming the immobilization processes

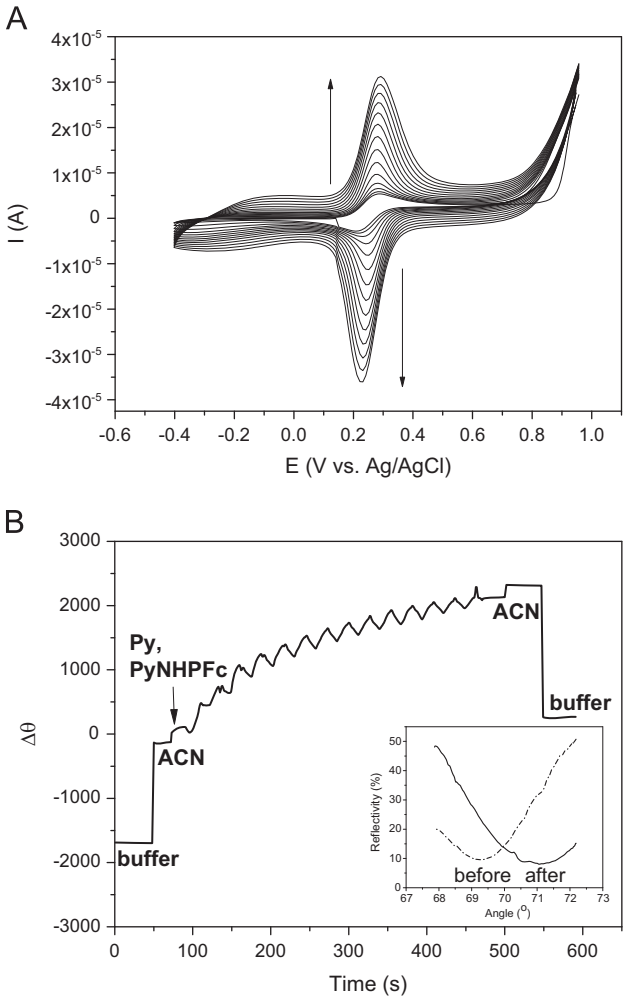

Fig. 2. Electrochemical and SPR characterization of copoly(Py-PyFcNHP) formation on the gold electrode. (A) CV curves obtained during polymerization of Py 8 mM and PyFcNHP 2 mM in acetonitrile containing 0.5 M $LiClO_4$ during 14 scans; (B) SPR kinetic curve obtained during the polymerization reaction in acetonitrile. Inset: reflectivity signals obtained in 10 mM PBS before and after polymerization.

of these two molecules (Fig. 3A). The amount of immobilized streptavidin was estimated to 1.42 ng mm^{-2}, and of biotinylated antibody Ab R14 to 0.4 ng mm^{-2}, according to the method developed by Stenberg et al. where 120 m° correspond to 1 ng mm^{-2} of protein coverage (Stenberg et al., 1991). On the basis of molecular weights of 60 and 120 kDa for streptavidin and biotinylated Ab R14 respectively, the surface concentration of streptavidin was estimated to 0.024 pmol mm^{-2} and the antibody to 0.003 pmol mm^{-2}. If we assume a three-to-one antibody/streptavidin binding ratio (streptavidin has four binding sites for biotin) and that SPR response is proportional to the bound amount, the stoichiometric ratio should have a value of 3. Strikingly, a ratio of only 0.125 was obtained. This suggests that probably not all biotin binding sites in immobilized streptavidin molecules are accessible for biotinylated antibody binding. Indeed, considering their respective molecular mass (120 vs 60 kDa), this one of antibody Ab R14 is 2 times higher compared to the streptavidin.

The surface topology of the modified gold electrode was studied using AFM technique in the contact mode. Fig. 3B (left panel) shows the copolymer copoly(PyPyFcNHP) topology where the roughness parameter was calculated as ca. 2.07 nm. Based on the profile of the surface, the thickness of the film of copolymer was estimated to 10 nm which confirmed the SPR estimation. A

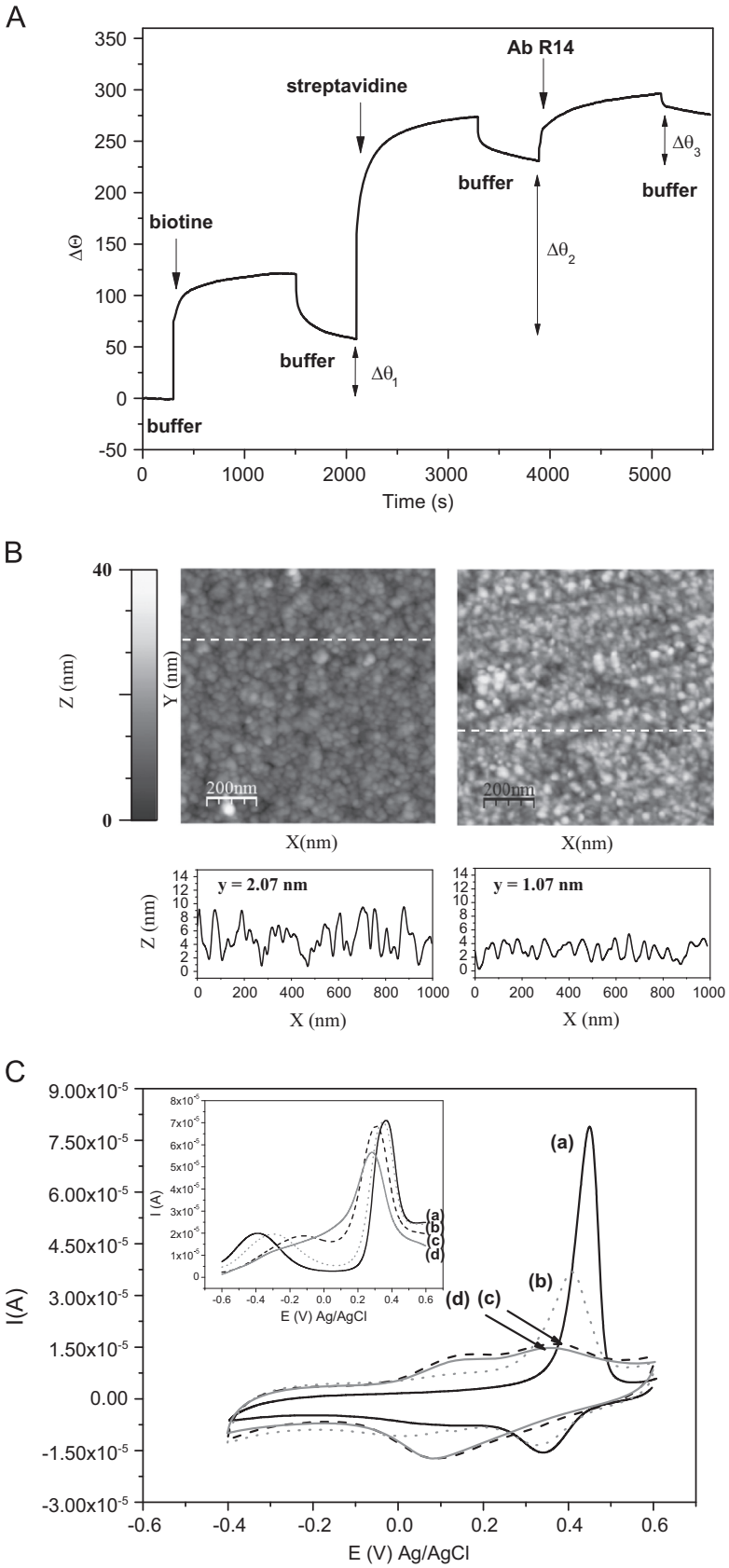

Fig. 3. Analysis of various steps of biolayer formation: (A) SPR kinetic curve of different steps of biosensor construction: immobilization of biotin hydrazide (2 mg mL^{-1}), streptavidin (100 μg mL^{-1}), and biotinylated antibody Ab R14 (8 μg mL^{-1}) followed by washing with PBS buffer; (B) topographic AFM image (1 μm × 1 μm) of (a) gold surface modified with copolypyrrole film and (b) after biotinyled Ab R14 antibody grafting; (C) CVs recorded and DPV measurements (inset) for (a) Step I: copoly(Py-PyNHP), (b) binding of biotin hydrazine, (c) immobilization of streptavidin, (d) immobilization of biotinyled Ab R14. PBS 10 mM, pH 7.4, scan rate 100 mV s^{-1}.

decrease of roughness factor from 2.07 to 1.07 nm was observed after immobilization of antibody Ab R14 (Fig. 3B, right panel). This indicates that the surface became more dense and homogenous and suggests a good organization and dispersion of molecules on the surface.

Biolayer formation was also followed by the electrochemical measurements. Fig. 3C exhibits the CV data obtained in PBS buffer solution for each step of the biolayer construction. Curve 3a shows the CV after polymer formation where redox signal is observed at potential of 0.45 V for oxidation and 0.33 V for reduction peaks. The redox signal can be attributed to the electrochemical response of both polypyrrole and ferrocene as it was previously characterized (Lê et al., 2010b). The successive addition of biomolecules onto the surface was accompanied by decrease in current density and shift of a maximum potential of the redox signal. As expected, the immobilization of the biomolecules changed redox properties by modifying environment of the copolymer layer. Similar feature was already demonstrated in the case of other biosensors based on modified polypyrrole with redox marker (Korri-Youssoufi and Makrouf, 2002; Bouchet et al., 2007; Chebil et al., 2013).

Faradaic currents of biosensor assembly were also investigated by the DPV technique (Fig. 3C, inset). DPV curves obtained after the copolymer formation discriminated the redox signal of polypyrrole from that of ferrocene at respectively −0.38 and 0.36 V. Indeed, the immobilization of the biomolecules on the surface modified with copoly(Py-PyFcNHP) led to a decrease in current. This could be related to the blocking effects for the charge transfer and penetration of the ions caused by large sizes of immobilized biomolecules on the surface (Chebil et al., 2010). Overall, SPR, AFM and electrochemical measurements demonstrated the efficient immobilization of the Ab R14 antibody on the biosensor surface.

3.3. Electrochemical detection of recombinant PB1-F2

The R14 antibody selectivity was studied with various proteins that are characterized by similar net charge and molecular weight (Shadoo, A-β and N-terminal part of prion protein) using SPR measurement. The antibody demonstrates high sensitivity only to PB1-F2 protein while no interaction was observed with control proteins (Vidic et al., 2013). The sensitivity of the biosensor was explored with recombinant PB1-F2 protein. The antibody/PB1-F2 interactions were monitored by CV and DPV measurement. Fig. 4A exhibits the CV data of biosensor obtained after incubation with various concentrations of PB1-F2 ranging from 5 nM to 5 μM. The current intensities of both reductive and oxidative peak decreased when the concentration of PB1-F2 is higher. The variations of the current were related to the amount of PB1-F2 bound to modified biolayer surface with Ab R14. Same behavior was observed with DPV measurement (Fig. 4B). These variations could be explained by the fact that formation of complex Ab R14/PB1-F2 prevents the penetration of ions on the sensor surface and blocks the charge transfer between electrode and ferrocene. Same behavior has been already demonstrated after antibody/antigen interaction measured with electrochemical transducer based on conducing polymers with redox markers (Piro et al., 2010).

The calibration curve was plotted based on the variation of current corresponding to the redox signal of ferrocenyl group at 0.4 V vs. Ag/AgCl, versus the concentration of PB1-F2 protein (Fig. 4C). The response exhibits a dynamic range of detection of PB1-F2 from 5 nM to 1.5 μM. Two linear curves were observed from the calibration curve, the first one from 50 nM to 300 nM and the second from 0.5 μM to 1.5 μM of PB1-F2 (Fig. 4C, inset). This is probably due to the two specific binding sites of the antibody: the first site of fixation is occupied by PB1-F2 at low protein concentrations while the second site seems to need higher PB1-F2 concentrations to interact with it. The saturation of biosensor was observed for 1.5 μM PB1-F2. The

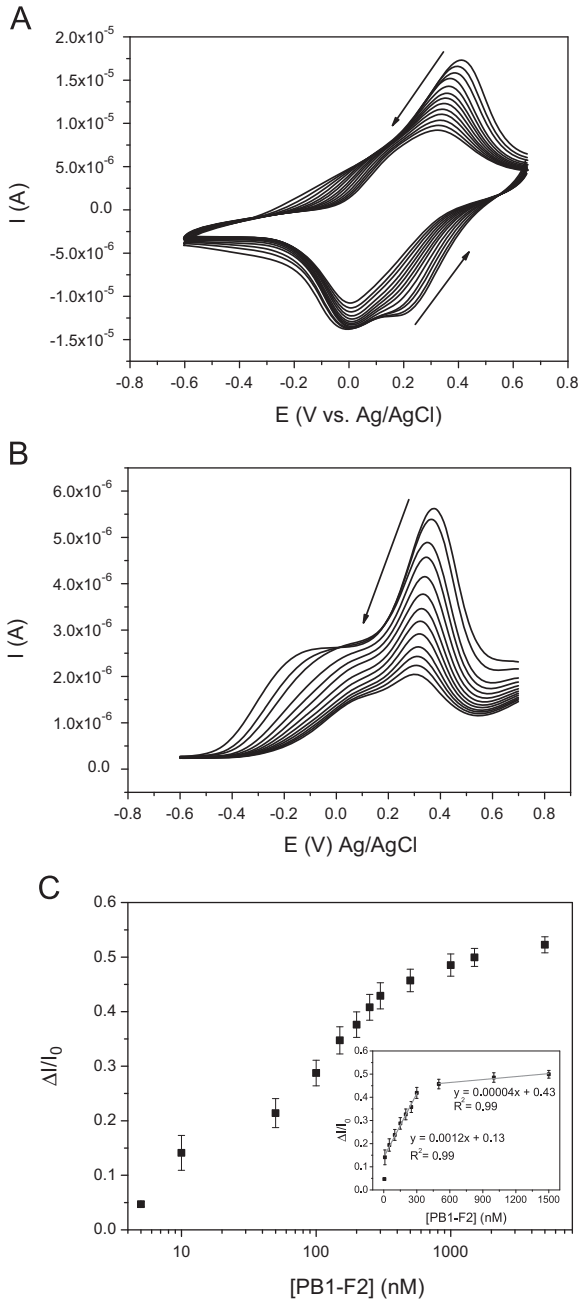

Fig. 4. Concentration–response curves for PB1-F2 protein specific detection in the range of concentrations: 5, 10, 50, 100, 150, 200, 250, 300, 500, 1000, 1500 and 5000 nM. (A) CVs and (B) DPVs obtained with successive additions of PB1-F2 in 5 mM sodium acetate buffer, pH 5. scan rate 100 mV s^{-1}. (C) Calibration curve showing the variation of current of ferrocene group as a function of the different concentrations of PB1-F2. Data points are the mean values obtained in 3 independent experiments ± SD.

detection limit was calculated from the first linear curve obtained at low concentration range. This was determined as 0.42 nM according UPAIC rules with formula ($3S_0/d$) where S_0 is the standard deviation of blank test measured with 3 biosensors as 0.012 and d is sensitivity deduced from the slope of the linear curve. The reproducibility of detection was tested with 3 independent measurements made with fresh prepared biosensors in all range of detected concentration of PB1-F2 protein. The relative standard deviation of such measurements, was determined as 1–3%, which demonstrates a highly reproducibility of the electrochemical biosensors.

3.4. Detection of PB1-F2 in infected cells

In order to study the efficiency of the biosensor to detect PB1-F2 in biological samples, A549 cells were infected with wild type virus (WT) or with its PB1-F2 knock-out mutant (F2). Lysates of F2-infected cells were used for signal background estimation since in this context all the cellular and the viral proteins are expressed except PB1-F2. Indeed, previous reports indicate that there is no significant difference of progeny virus titers between wild type and PB1-F2 knock out F2 virus upon infection of various cell lines (Chevalier et al., 2010; LE Goffic et al., 2011). The second negative control was lysates of non-infected cells.

Cells were collected at 4, 6, 8 and 24 h post-infection. The biosensors with immobilized Ab R14 antibody were immersed into the solutions containing cell lysates for 40 min. Then, the sensor surface was washed with 5 mM sodium acetate pH 5 buffer to eliminate non-bound proteins. Fig. 5A illustrates the CV signals recorded by the biosensor before (solid) and after (dash) application of WT-infected cell lysates at 8 h post-infection. The reduction of the current reflects the antigen/antibody interactions that prevent charge transfer and ions penetration. In contrast, biosensor incubation with lysates of either non-infected (NI) cells or F2-infected cells showed no significant variation of the current pointing out the absence of non-specific binding of the others proteins presents in lysates (Figs. 5B and C, respectively). This undergoes the specificity and selectivity of this biosensor to PB1-F2 proteins produced in WT-infected cells and any interactions with others proteins present in cells.

The concentration of PB1-F2 in WT-infected cells was evaluated by reporting the variation of the ferrocene current to the calibration curve presented in Fig. 4C. The results are presented as the mean $\pm$ standard deviation of 4 separate experiments in different lysates. At early stage of infection (4 h post-infection), PB1-F2 was barely detectable suggesting that protein expression started then. The quantity of PB1-F2 increases after 6 h post-infection (88 ± 1 pmol mg^{-1}) to reach the highest concentration at 8 h post-infection (374 ± 20 pmol mg^{-1}). PB1-F2 was not detected at 24 h post-infection.

The results obtained clearly showed that the concentration of PB1-F2 protein varies during viral cycle and reach its maximum at 8 h post-infection. This is in accordance with previous studies that reported the transitional expression of PB1-F2 in infected cells and tissues (Chen et al., 2001; Le Goffic et al., 2010, Vidic et al., 2013). However, PB1-F2 was shown to polymerize into amyloid fibers in infected cells (Chevalier et al., 2010). In consequence, the sensor failure to detect PB1-F2 at 24 h post-infection could be explained either by its generally accepted short half-life or by its recruitment as monomers to form amyloid fibers or aggregates in the late stage of infection.

To the best of our knowledge this immunosensor is the first electrochemical device reported for detection of a nonstructural IAV protein. In literature, most works concern the detection of IAV structural proteins as HA and NA with the aim to develop new diagnostic tools. For instance, CdS quantum dots-based biosensor with glycan receptor binding immobilized on the nanoparticle through streptavidin has been developed to detect H5N1 (Krejcova et al., 2012). Field effect transistors (FET) biosensor technology was applied to distinguish HA molecules between their human and avian subtypes and lead to detection limit of 50 pM (Hideshima et al., 2013). Improvement of detection, until at attomolar level, was demonstrated by the same authors using trisaccharide as a bioreceptor. Another work reported a biosensor based on magnetic beads modified by α-H5 and α-N1 antibodies that specifically detected AIV H5N1 subtypes (Lum et al., 2012).

Furthermore, regarding non-structural IAV proteins, which are not incorporated into the mature virion, there are less disposable sensible analytical tools for their quantification and study. Classical diagnostic tests are based on the immunological detection of antigens such as NS1 which is expressed in large amount in the infected cells (Jian-Umpunkul et al., 2012). In contrast, conventional immunological tests such as Western blot analysis and ELISA have a low analytical sensitivity to study PB1-F2 expression during the viral cycle. Furthermore, highly sensitive RT-PCR test does not allow quantifying PB1-F2 since the mRNA is not necessarily correlated to the expressed protein (Chen et al., 2010). Here we present the potentiality of electrochemical

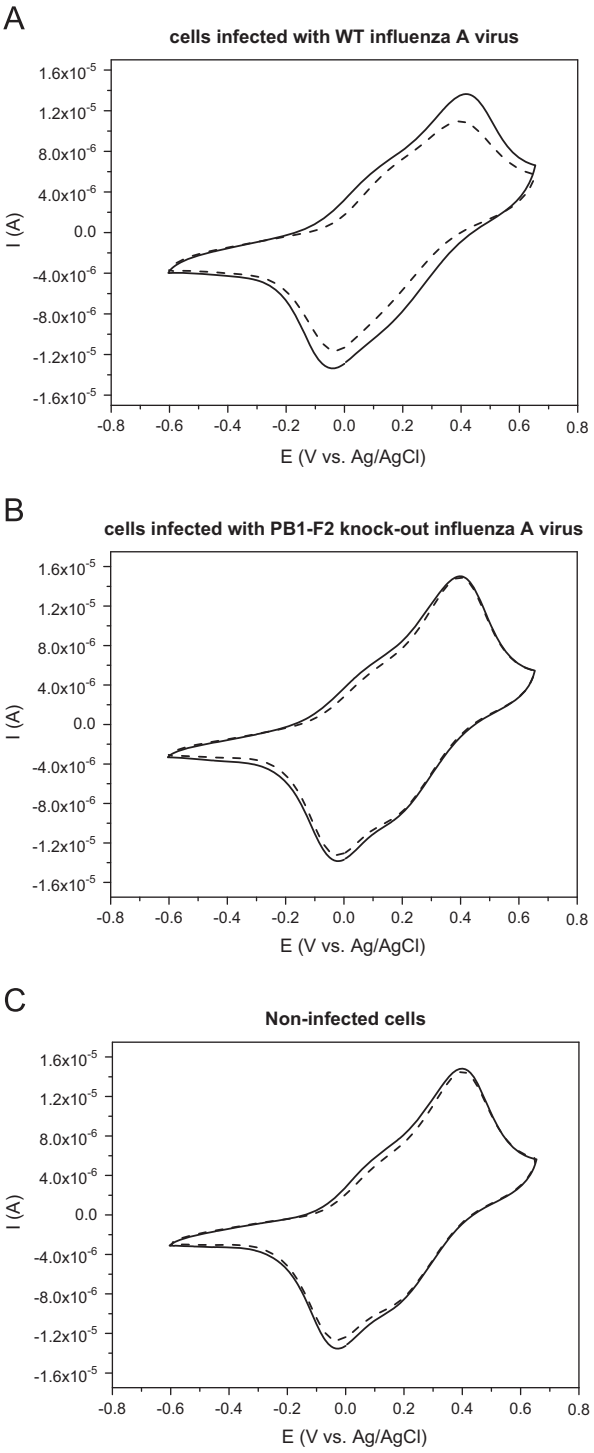

Fig. 5. Curves obtained before (solid line) and after (dash line) detection of PB1-F2 in IAV-infected epitephial human cell line A549: (A) cells infected with WT influenza A virus expressing PB1-F2 protein; (B) cells infected with PB1-F2 knock-out influenza A virus mutant not-expressing PB1-F2; (C) non-infected cells.

immunosensor for detection of PB1-F2 protein in infected cell during viral cycle. Electrochemical biosensor allows fast and highly specific protein quantification during viral cycle. In addition, no labeling or special sample treatment is needed. Furthermore, this electrochemical biosensor can potentially be miniaturized. The application of such electrochemical biosensor device can be generalize to detect other IAV proteins associated to infected cells.

4. Conclusion

We have developed a sensitive electrochemical immunosensor based on polypyrrole and ferrocenyl group as a redox marker for detection and quantification of PB1-F2 protein in biological samples. PB1-F2 protein concentration was determined in IAV-infected cells through immunodetection system by measuring variation in redox signals of grafted ferrocene. Our results demonstrate that the electrochemical immunosensor can be used for quantitative detection of PB1-F2 protein at various times post-infection. The biosensor can thus be applied to follow PB1-F2 expression profile and to get insight into its molecular mechanism of action during the virus cycle. Results obtained open the way of using this electrochemical biosensor technology to detect other viral proteins in infected cells, tissues or biological samples and thus could lead to development of a new diagnostic tool for an IAV infection.

Acknowledgments

This work was supported by France Government CNRS and INRA institutions and we would like to thank Ministry of Higher Education and Research for Anna Miodek Graduate *Research* Fellowship. We are grateful to Charles-Adrien Richard for purification of PB1-F2 protein.

Appendix A. Supplementary Information

Supplementary data associated with this article can be found in the online version at http://dx.doi.org/10.1016/j.bios.2014.02.037.

References

Bouchet, A., Chaix, C., Marquette, C.A., Blum, L.J., Mandrand, B., 2007. Biosens. Bioelectron. 23 (5), 735–740.
Chebil, S., Hafaiedh, I., Sauriat-Dorizon, H., Jaffrezic-Renault, N., Errachid, A., Ali, Z., Korri-Youssoufi, H., 2010. Biosens. Bioelectron. 26 (2), 736–742.
Chebil, S., Miodek, A., Ambike, V., Sauriat-Dorizon, H., Policar, C., Korri-Youssouf, H., 2013. Sens. Actuators B 185, 762–770.
Chen, W., Calvo, P.A., Malide, D., Gibbs, J., Schubert, U., Bacik, I., Basta, S., O'Neill, R., Schickli, J., Palese, P., Henklein, P., Bennink, J.R., Yewdell, J.W., 2001. Nat. Med. 7 (12), 1306–1312.
Chen, C.J., Chen, G.W., Wang, C.H., Huang, C.H., Wang, Y.C., Shih, S.R., 2010. J. Virol. 84 (19), 10051–10062.
Chung, D.-J., Kim, K.-C., Choi, S.-H., 2011. Appl. Surf. Sci. 257 (22), 9390–9396.
Chevalier, C., Al Bazzal, A., Vidic, J., Février, V., Bourdieu, C., Bouguyon, E., LeGoffic, R., Vautherot, J.F., Bernard, J., Moudjou, M., Noinville, S., Chich, J.F., Da Costa, B., Rezaei, H., Delmas, B., 2010. J. Biol. Chem. 285 (17), 13233–13243.
Hideshima, S., Hinou, H., Ebihara, D., Sato, R., Kuroiwa, S., Nakanishi, T., Nishimura, S.I., Osaka, T., 2013. Anal. Chem. 85 (12), 5641–5644.
Jian-umpunkul, P., Thepthai, C., Apiwat, N., Chantima, W., Poomputsa, K., Wiriya-chaiporn, N., Dharakul, T., 2012. J. Virol. Methods 185 (1), 24–31.
Kamikawa, T.L., Mikolajczyk, M.G., Kennedy, M., Zhang, P., Wang, W., Scott, D.E., Alocilja, E.C., 2010. Biosens. Bioelectron. 26 (4), 1346–1352.
Kao, L.T.H., Shankar, L., Kang, T.G., Zhang, G., Tay, G.K.I., Rafei, S.R.M., Lee, C.W.H., 2011. Biosens. Bioelectron. 26 (5), 2006–2011.
Korri-Youssoufi, H., Makrouf, B., 2002. Anal. Chem. Acta 469 (1), 85–92.
Krejcova, L., Dospivova, D., Ryvolova, M., Kopel, P., Hynek, D., Krizkova, S., Hubalek, J., Adam, V., Kizek, R., 2012. Electrophoresis 33 (21), 3195–3204.
Kukol, A., Li, P., Estrela, P., Ko-Ferrigno, P., Migliorato, P., 2008. Anal. Biochem. 374 (1), 143–153.
Lê, H.Q.A., Sauriat-Dorizon, H., Korri-Youssoufi, H., 2010a. Anal. Chim. Acta 674 (1), 1–8.
Lê, H.Q.A., Chebil, S., Makrouf, B., Sauriat-Dorizon, H., Mandrand, B., Korri-Youssoufi, H., 2010b. Talanta 81 (4–5), 1250–1257.
Le Goffic, R., Bouguyon, E., Chevalier, C., Vidic, J., Da Costa, B., Leymarie, O., Bourdieu, C., Decamps, L., Dhorne-Pollet, S., Delmas, B, 2010. J. Immunol. 185 (8), 4812–4823.
Le Goffic, R., Leymarie, O., Chevalier, C., Rebours, E., Da Costa, B., Vidic, J., Descamps, D., Sallenave, J.M., Rauch, M., Samson, M., Delmas, B., 2011. PLoS Pathog. 7 (8), e1002202.
Liu, X., Cheng, Z., Fan, Z., Aia, S., Han, R., 2011. Electrochim. Acta 56 (18), 6266–6270.
Lum, J., Wang, R., Lassiter, K., Srinivasan, B., Abi-Ghanem, D., Berghman, L., Hargis, B., Tung, S., Lu, H., Li, Y., 2012. Biosens. Bioelectron. 38 (1), 67–73.
Palese, P., 1977. Cell 10 (1), 1–10.
Pavlovic, E., Lai, R.Y., Wu, T.T., Ferguson, B.S., Sun, R., Plaxco, K.W., Soh, H.T., 2008. Langmuir 24 (3), 1102–1107.
Piro, B., Zhang, Q.D., Reisberg, S., Noel, V., Dang, L.A., Duc, H.T., Pham, M.C., 2010. Talanta 82 (2), 608–612.
Stenberg, E., Persson, B., Roos, H., Urbaniczky, C., 1991. J. Colloid Interface Sci. 143 (2), 513–526.
Tam, P.D., Van Hieu, N., Chien, N.D., Le, A.-T., Anh Tuan, M., 2009. J. Immunol. Methods 350 (1–2), 118–124.
Vidic, J., Chevalier, C., Le Goffic, R., Miodek, A., Bourdieu, C., Richard, C.-A., Moudjou, M., Delmas, B., 2013. J. Anal. Bioanal. Tech., S7, http://dx.doi.org/10.4172/2155-9872.S7-006.
Yewdell, J.W., Ince, W.L., 2012. Science 337 (6091), 164–165.
Wang, R., Wang, Y., Lassitera, K., Li, Y., Hargis, B., Tung, S., Berghmand, L., Bottje, W., 2009. Talanta 79 (2), 159–164.
Wang, R., Lin, J., Lassiter, K., Srinivasan, B., Lin, L., Lu, H., Tung, S., Hargis, B., Bottje, W., Berghman, L., Li, Y., 2011. J. Virol. Methods 178 (1–2), 52–58.
Wise, H.M., Barbezange, C., Jagger, B.W., Dalton, R.M., Gog, J.R., Curran, M.D., Taubenberger, J.K., Anderson, E.C., Digard, P., 2011. Nucleic Acids Res. 39 (17), 7775–7790.
Zhu, X., Ai, S., Chen, Q., Yin, H., Xu, J., 2009. Electrochem. Commun. 11 (7), 1543–1546.